RATE ANALYSIS OF SPATIAL MULTIPLEXING IN MIMO HETEROGENEOUS NETWORKS WITH WIRELESS BACKHAUL

Howard H. Yang, Giovanni Geraci, and Tony Q. S. Quek

Singapore University of Technology and Design

ABSTRACT

In this paper, we develop a general framework to analyze the rate performance of a two-tier MIMO heterogeneous network (HetNet) with wireless backhaul under spatial multiplexing. We consider linear precoding and receive filtering in the presence of interference from uplink and downlink transmissions. We find that the sum rate per area of the HetNet is sensitive to the network load, i.e., the number of users served by each base station. We show that a two-tier HetNet with wireless backhaul can achieve higher sum rate per area than a one-tier cellular network. However, this requires the bandwidth division between radio access links and wireless backhaul to be optimally designed according to the load conditions.

***Index Terms*—** Heterogeneous cellular networks, MIMO, wireless backhaul, spatial multiplexing, linear precoding.

1. INTRODUCTION

In order to meet the exponentially growing mobile data demand, heterogeneous networks (HetNets) are being deployed for the next generation of wireless communication systems [1, 2]. HetNets will provide higher coverage and throughput by overlaying macro cells with a large number of small cells and access points, thus offloading traffic and reducing the distance between transmitter and receiver [3–5].

When small cells are densely deployed, it becomes necessary to aggregate a massive cellular traffic from small cell access points (SAPs) towards macro base stations (MBSs), and a wireless backhaul is regarded as the only practical solution for outdoor scenarios where wired links are not available [6, 7]. A dense deployment of small cells that use a wireless backhaul will shift the design challenge from the radio access links to the backhaul, which can thus be identified as the new bottleneck of the network [8].

Therefore, it is critically important to investigate how employing a wireless backhaul to connect SAPs and MBSs affects the overall network performance. Despite a growing interest from the research community [9–11], the current literature still lacks a general study that encompasses all the key features of a HetNet, namely interference from uplink (UL) and downlink (DL) transmissions, spatial multiplexing, limited backhaul capacity, and random channels and topology.

In this paper, we study the sum rate per area of a MIMO HetNet with wireless backhaul under spatial multiplexing. We develop an analytical framework that combines tools from random matrix theory and stochastic geometry. Our analysis is general and accounts for linear precoding and receive filtering, UL/DL transmissions, interference, load, and deployment strategy. We quantify the impact of several network parameters on the rate, thus providing useful design insights. Our main contribution are summarized as follows.

- We provide a general toolset to analyze the rate of a two-tier MIMO HetNet with wireless backhaul. Our model accounts for both UL and DL transmissions and spatial multiplexing, for the bandwidth and power allocated between macro cells, small cells, and backhaul, and for the infrastructure deployment strategy.
- We find that, under spatial multiplexing, the rate is sensitive to the load conditions of the network, thus establishing the importance of scheduling the right number of UEs per base station when linear schemes are employed for precoding and receive filtering.
- We show that in certain scenarios, a two-tier HetNet with wireless backhaul can exhibit a significant performance gain over a one-tier cellular network. However, this requires the backhaul bandwidth to be optimally allocated according to the load conditions of the network.

2. SYSTEM MODEL

We study a two-tier HetNet which consists of MBSs, SAPs, and user equipments (UEs), as depicted in Fig. 1. The spatial locations of MBSs, SAPs, and UEs follow independent PPPs Φ_{m}, Φ_{s}, and Φ_{u}, with spatial densities λ_{m}, λ_{s}, and λ_{u}, respectively. All MBSs, SAPs, and UEs transmit with power P_{mt}, P_{st}, and P_{ut}, and are equipped with M_{m}, M_{s}, and 1 antennas, respectively. Each UE associates with the base station that provides the largest average received power, and each SAP associates with the closest MBS. The links between MBSs-UEs, SAPs-UEs, and MBSs-SAPs are referred to as *macro*

This work was supported in part by the SUTD-ZJU Research Collaboration under Grant SUTD-ZJU/RES/01/2014 and the MOE ARF Tier 2 under Grant MOE2014-T2-2-002.

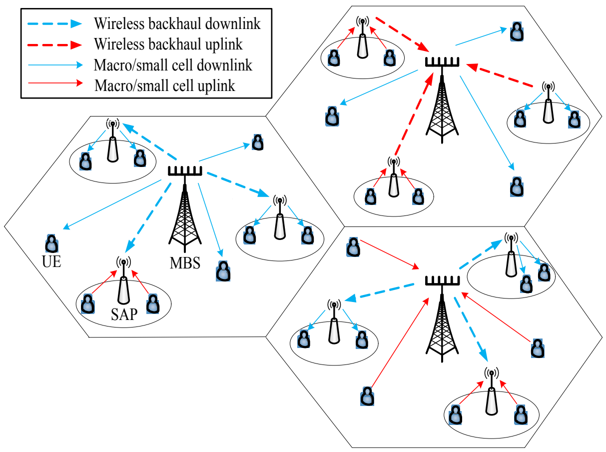

Fig. 1. Illustration of a two-tier heterogeneous network with wireless backhaul.

cells, *small cells*, and *backhaul*, respectively. We approximate the number of UEs and SAPs associated to a MBS, as well as the number of UEs associated to a SAP by constant values K_{m}, K_{b}, and K_{s}, respectively. In light of its higher spectral efficiency [12], we consider spatial multiplexing where each MBS and each SAP simultaneously serve K_{m} and K_{s} UEs, respectively, and each MBS simultaneously serves K_{b} SAPs on the backhaul. We assume $K_{\mathrm{m}} \leq M_{\mathrm{m}}$, $K_{\mathrm{s}} \leq M_{\mathrm{s}}$, and $K_{\mathrm{b}} M_{\mathrm{s}} \leq M_{\mathrm{m}}$, due to spatial multiplexing limitations [13]. The load on macro cells, small cells, and backhaul is denoted by $\beta_{\mathrm{m}} = \frac{K_{\mathrm{m}}}{M_{\mathrm{m}}}$, $\beta_{\mathrm{s}} = \frac{K_{\mathrm{s}}}{M_{\mathrm{s}}}$, and $\beta_{\mathrm{b}} = \frac{K_{\mathrm{b}} M_{\mathrm{s}}}{M_{\mathrm{m}}}$, respectively.

In this work, we consider a co-channel deployment of small cells with the macro cell tier, i.e., macro cells and small cells share the same frequency band for transmission. As opposed to non-co-channel deployments, this provides higher efficiency and better spectrum utilization [14]. We further consider an out-of-band wireless backhaul [6], i.e., the total available bandwidth is divided into two portions, where a fraction ζ_{b} is used for the wireless backhaul, and the remaining $(1 - \zeta_{\mathrm{b}})$ is shared by the radio access links (macro cells and small cells). In order to adapt the radio resources to the variation of the DL/UL traffic demand, we assume that MBSs and SAPs operate in a dynamic time division duplex (TDD) mode [14], where at every time slot, all MBSs and SAPs independently transmit in downlink with probabilities τ_{m}, τ_{s}, and τ_{b} on the macro cell, small cell, and backhaul, respectively, and they operate in uplink for the remaining time. We model the channels between any pair of antennas in the network as independent, narrowband, and affected by two attenuation components, namely small-scale Rayleigh fading and large-scale path loss, where α is the path loss exponent, and by thermal noise with variance σ^2. We assume that all MBSs and SAPs use a zero forcing (ZF) scheme for both transmission and reception, due to its practical simplicity [15, 16].

3. RATE ANALYSIS

In this section, we analyze the data rates of a HetNet with wireless backhaul, by first deriving all uplink and downlink rates on macro cells, small cells, and backhaul. Unless otherwise stated, the analytical expressions provided in this section are tight approximations of the actual data rates. Due to the page limit, some proofs and mathematical derivations have been omitted. These can be found in [17], along with several simulation results that confirm the accuracy of the analysis and approximations presented in this section.

By noting that in practice MBSs are equipped with a relatively large number of antennas, we can use random matrix theory tools to obtain the rate on a macro cell link [18–20].

Lemma 1. *The DL and UL rates on a macro cell are*

$$R_{\mathrm{m}}^{\mathrm{DL}} = (1-\zeta_{\mathrm{b}}) \int_0^\infty \int_0^\infty \int_0^\infty \log_2 \left[1 + \frac{P_{\mathrm{mt}} (1-\beta_{\mathrm{m}}) (G_{\mathrm{m}} \pi)^{\frac{\alpha}{2}}}{\beta_{\mathrm{m}} \Gamma\left(1+\frac{\alpha}{2}\right) (\sigma^2 + x + z)} \right] f_{I_1}(x,t)\, f_{I_{\mathrm{u}}}(z)\, f_{r_{\mathrm{m}}}(t)\, dx\, dz\, dt \quad (1)$$

$$R_{\mathrm{m}}^{\mathrm{UL}} = (1-\zeta_{\mathrm{b}}) \int_0^\infty \int_0^\infty \log_2 \left[1 + \frac{P_{\mathrm{mt}} M_{\mathrm{m}} (1-\beta_{\mathrm{m}}) t^{-\alpha}}{\sigma^2 + x} \right] f_{I_2}(x)\, f_{r_{\mathrm{m}}}(t)\, dx\, dt \quad (2)$$

with $f_{I_{\mathrm{u}}}(x)$, $f_{I_1}(x)$, $f_{I_2}(x)$, $f_{r_{\mathrm{m}}}(t)$, *and* G_{m} *given by* (4), (5), (12), (9), *and* (10).

Proof. Consider a typical UE located at the origin with its serving MBS at c. Under dynamic TDD, the deterministic equivalent of the downlink SINR can be written as [21]

$$\gamma_{\mathrm{m}}^{\mathrm{DL}} \to \bar{\gamma}_{\mathrm{m}}^{\mathrm{DL}} = \frac{P_{\mathrm{mt}} (1-\beta_{\mathrm{m}}) (G_{\mathrm{m}} \pi)^{\frac{\alpha}{2}}}{\beta_{\mathrm{m}} \Gamma\left(1+\frac{\alpha}{2}\right) (I_1 + I_{\mathrm{u}} + \sigma^2)}, \quad a.s. \quad (3)$$

with I_1 and I_{u} the aggregate interference from MBSs and SAPs and the interference from UEs, respectively. The probability density function (pdf) of I_{u} can be approximated as [22]

$$f_{I_{\mathrm{u}}}(x) = \frac{\tilde{\lambda}_{\mathrm{u}} P_{\mathrm{ut}}^{\frac{2}{\alpha}}}{4} \left(\frac{\pi}{x}\right)^{\frac{3}{2}} \exp\left(-\frac{\pi^4 P_{\mathrm{ut}}^{\frac{4}{\alpha}} \tilde{\lambda}_{\mathrm{u}}^2}{16x} \right) \quad (4)$$

where $\tilde{\lambda}_{\mathrm{u}} = (1-\tau_{\mathrm{m}}) \lambda_{\mathrm{m}} K_{\mathrm{m}} + (1-\tau_{\mathrm{s}}) \lambda_{\mathrm{s}} K_{\mathrm{s}}$. Conditioned on $\|c\| = t$, the pdf of I_1 can be approximated as [23]

$$f_{I_1}(x,t) = e^{-\frac{\left(\log x - \mu_{I_1,N}(t)\right)^2}{2\sigma^2_{I_1,N}(t)}} \cdot \left[\sqrt{2\pi} x \sigma_{I_1,N}(t)\right]^{-1}, \; x > 0 \quad (5)$$

where $\mu_{I_1,N}(t) = \log \mu_{I_1}(t) - 0.5 \log\left(1 + \sigma^2_{I_1}(t)/\mu^2_{I_1}(t)\right)$ and $\sigma_{I_1,N}(t) = \log\left(1 + \sigma^2_{I_1}(t)/\mu^2_{I_1}(t)\right)$, with $\mu_{I_1}(t)$ and $\sigma^2_{I_1}(t)$ given by $\mu_{I_1}(t) = P_{\mathrm{mt}} G_{\mathrm{m}} 2\pi t^{-(\alpha-2)}/\alpha - 2$ and

$$\sigma^2_{I_1}(t) = \frac{P^2_{\mathrm{mt}} \pi t^{-2(\alpha-1)}}{\alpha - 1} \left[G_{\mathrm{m}} + \frac{\tau_{\mathrm{m}} \lambda_{\mathrm{m}}}{K_{\mathrm{m}}} + \frac{\tau_{\mathrm{s}} \lambda_{\mathrm{s}}}{K_{\mathrm{s}}} \left(\frac{P_{\mathrm{st}}}{P_{\mathrm{mt}}}\right)^{\frac{2}{\alpha}} \right]. \quad (6)$$

Under the association rule defined in Section 2, the probability that a UE associates with a MBS or SAP can be respectively calculated as [3]

$$A_{\mathrm{m}} = \tau_{\mathrm{m}}\lambda_{\mathrm{m}}P_{\mathrm{mt}}^{\frac{2}{\alpha}} / \left(\tau_{\mathrm{m}}\lambda_{\mathrm{m}}P_{\mathrm{mt}}^{\frac{2}{\alpha}} + \tau_{\mathrm{s}}\lambda_{\mathrm{s}}P_{\mathrm{st}}^{\frac{2}{\alpha}}\right), \tag{7}$$

$$A_{\mathrm{s}} = \tau_{\mathrm{s}}\lambda_{\mathrm{s}}P_{\mathrm{st}}^{\frac{2}{\alpha}} / \left(\tau_{\mathrm{m}}\lambda_{\mathrm{m}}P_{\mathrm{mt}}^{\frac{2}{\alpha}} + \tau_{\mathrm{s}}\lambda_{\mathrm{s}}P_{\mathrm{st}}^{\frac{2}{\alpha}}\right). \tag{8}$$

As such, the pdf of $\|c\| = r_{\mathrm{m}}$ can be obtained as [3]

$$f_{r_{\mathrm{m}}}(r) = \frac{2\pi\tau_{\mathrm{m}}\lambda_{\mathrm{m}}r}{A_{\mathrm{m}}}\exp\left(-G_{\mathrm{m}}\pi r^2\right),\ r \geq 0 \tag{9}$$

$$G_{\mathrm{m}} = \tau_{\mathrm{m}}\lambda_{\mathrm{m}} + \tau_{\mathrm{m}}\lambda_{\mathrm{m}}\left(\frac{P_{\mathrm{mt}}}{P_{\mathrm{st}}}\right)^{\frac{2}{\alpha}}. \tag{10}$$

The DL rate then follows by using the continuous mapping theorem. The deterministic equivalent for the UL SINR is

$$\gamma_{\mathrm{m}}^{\mathrm{UL}} \to \bar{\gamma}_{\mathrm{m}}^{\mathrm{UL}} = \frac{P_{\mathrm{ut}}|M_{\mathrm{m}}(1-\beta_{\mathrm{m}})|\|c\|^{-\alpha}}{\sigma^2 + I_2}, \quad a.s. \tag{11}$$

where $I_2 = I_1 + I_{\mathrm{u}}$. We approximate the pdf of I_2 as [22]

$$f_{I_2}(x) = \frac{\lambda_{I_2}}{4}\left(\frac{\pi}{x}\right)^{\frac{3}{2}}\exp\left(-\frac{\pi^4\lambda_{I_2}^2}{16x}\right) \tag{12}$$

where $\lambda_{I_2} = \tilde{\lambda}_{\mathrm{u}}P_{\mathrm{ut}}^{\frac{2}{\alpha}} + \lambda_{K_{\mathrm{m}}}P_{\mathrm{mt}}^{\frac{2}{\alpha}}/K_{\mathrm{m}}^{\frac{2}{\alpha}} + \lambda_{K_{\mathrm{s}}}P_{\mathrm{st}}^{\frac{2}{\alpha}}/K_{\mathrm{s}}^{\frac{2}{\alpha}}$ with $\lambda_{K_{\mathrm{m}}} = \tau_{\mathrm{m}}\lambda_{\mathrm{m}}\Gamma\left(1+\frac{2}{\alpha}\right)\prod_{i=1}^{K_{\mathrm{m}}-1}\left(i+\frac{2}{\alpha}\right)/\Gamma(K_{\mathrm{m}})$ and $\lambda_{K_{\mathrm{s}}} = \tau_{\mathrm{s}}\lambda_{\mathrm{s}}\Gamma\left(1+\frac{2}{\alpha}\right)\prod_{i=1}^{K_{\mathrm{s}}-1}\left(i+\frac{2}{\alpha}\right)/\Gamma(K_{\mathrm{s}})$. The UL rate follows from (11), (12), and the continuous mapping theorem. □

Next, using the effective channel distribution, we derive the uplink and downlink rates for the small cell as follows.

Lemma 2. *The DL and UL rates on a small cell are given by*

$$R_{\mathrm{s}}^{\mathrm{DL}} = (1-\zeta_{\mathrm{b}})\int_0^\infty\int_0^\infty\int_0^\infty\int_0^\infty \log_2\left(1+\frac{P_{\mathrm{st}}vt^{-\alpha}}{\sigma^2+x+y}\right) f_{I_3}(x,t)\, f_{I_{\mathrm{u}}}(y)\, f_{r_{\mathrm{s}}}(t)\, f_v(v)\, dx\, dy\, dt\, dv \tag{13}$$

$$R_{\mathrm{s}}^{\mathrm{UL}} = (1-\zeta_{\mathrm{b}})\int_0^\infty\int_0^\infty\int_0^\infty \log_2\left(1+\frac{P_{\mathrm{st}}vt^{-\alpha}}{\sigma^2+x}\right) f_v(v)\, f_{r_{\mathrm{s}}}(t)\, f_{I_2}(x)\, dv\, dx\, dt \tag{14}$$

where $f_v(v)$ follows a gamma distribution given by $f_v(v) = x^{\Delta_{\mathrm{s}}-1}e^{-x}/\Gamma(\Delta_{\mathrm{s}})$, with $\Delta_{\mathrm{s}} = M_{\mathrm{s}} - K_{\mathrm{s}} + 1$, and $f_{I_3}(x,t)$ and $f_{r_{\mathrm{s}}}(t)$ are given by

$$f_{I_3}(x,t) = \frac{e^{-\frac{\left(\log x - \mu_{I_3,N}(t)\right)^2}{2\sigma_{I_3,N}^2(t)}}}{\sqrt{2\pi}x\sigma_{I_3,N}(t)},\ \ x > 0 \tag{15}$$

$$f_{r_{\mathrm{s}}}(r) = \frac{2\pi\tau_{\mathrm{s}}\lambda_{\mathrm{s}}r}{A_{\mathrm{s}}}\exp\left(-G_{\mathrm{s}}\pi r^2\right),\ r \geq 0 \tag{16}$$

where $G_{\mathrm{s}} = \tau_{\mathrm{s}}\lambda_{\mathrm{s}} + \tau_{\mathrm{m}}\lambda_{\mathrm{m}}\left(P_{\mathrm{mt}}/P_{\mathrm{st}}\right)^{\frac{2}{\alpha}}$ and $\mu_{I_3,N}(t) = \log\mu_{I_3}(t) - 0.5\log\left(1+\sigma_{I_3}^2(t)/\mu_{I_3}^2(t)\right)$ and $\sigma_{I_3,N}(t) = \log\left(1+\sigma_{I_3}^2(t)/\mu_{I_3}^2(t)\right)$, with $\mu_{I_3}(t)$ and $\sigma_{I_3}^2(t)$ given by $\mu_{I_3}(t) = P_{\mathrm{st}}G_{\mathrm{s}}2\pi t^{-(\alpha-2)}/(\alpha-2)$ and

$$\sigma_{I_3}^2(t) = \frac{P_{\mathrm{st}}^2\pi t^{2(1-\alpha)}}{\alpha-1}\left[G_{\mathrm{s}} + \frac{\tau_{\mathrm{s}}\lambda_{\mathrm{s}}}{K_s} + \frac{\tau_{\mathrm{m}}\lambda_{\mathrm{m}}}{K_m}\left(\frac{P_{\mathrm{mt}}}{P_{\mathrm{st}}}\right)^{\frac{2}{\alpha}}\right]. \tag{17}$$

Proof. See [17] for a detailed proof. □

More compact upper and lower bounds on (13) can be found in [17]. We now derive downlink and uplink rates on the wireless backhaul of a HetNet as follows.

Lemma 3. *The DL and UL rates on the wireless backhaul are*

$$R_{\mathrm{b}}^{\mathrm{DL}} = \frac{\zeta_{\mathrm{b}}M_{\mathrm{s}}}{K_{\mathrm{s}}}\int_0^\infty\int_0^\infty\int_0^\infty \log_2\left[1+\frac{P_{\mathrm{mb}}(1-\beta_{\mathrm{b}})\left(\tau_{\mathrm{b}}\lambda_{\mathrm{m}}\right)^{\frac{\alpha}{2}}}{\beta_{\mathrm{b}}\Gamma(1+\frac{\alpha}{2})(\sigma^2+x+y)}\right] f_{I_{\mathrm{m}}}(x,t)\, f_{I_{\mathrm{s}}}(y)\, f_{r_{\mathrm{b}}}(t)\, dx\, dy\, dt \tag{18}$$

$$R_{\mathrm{b}}^{\mathrm{UL}} = \frac{\zeta_{\mathrm{b}}M_{\mathrm{s}}}{K_{\mathrm{s}}}\int_0^\infty\int_0^\infty \log_2\left[1+\frac{P_{\mathrm{sb}}M_{\mathrm{m}}(1-\beta_{\mathrm{b}})}{(\sigma^2+x)t^{\alpha}}\right] f_{I_4}(x)\, f_{r_{\mathrm{b}}}(t)\, dx\, dt \tag{19}$$

where $f_{r_{\mathrm{b}}}(t) = 2\pi\tau_{\mathrm{b}}\lambda_{\mathrm{m}}t\exp\left(-\pi\tau_{\mathrm{b}}\lambda_{\mathrm{m}}t^2\right)$, $f_{I_{\mathrm{m}}}(x,t)$, $f_{I_{\mathrm{s}}}(y)$, and $f_{I_4}(x)$ are given as follows

$$f_{I_{\mathrm{m}}}(x,t) = e^{-\frac{\left(\log x - \mu_{I_{\mathrm{m}},N}(t)\right)^2}{2\sigma_{I_{\mathrm{m}},N}^2(t)}}\left[\sqrt{2\pi}x\sigma_{I_{\mathrm{m}},N}(t)\right]^{-1} \tag{20}$$

$$f_{I_{\mathrm{s}}}(x) = \frac{\lambda_{M_{\mathrm{s}}}P_{\mathrm{sb}}^{\frac{2}{\alpha}}}{4}\left(\frac{\pi}{x}\right)^{\frac{3}{2}}\exp\left(-\frac{\pi^4P_{\mathrm{sb}}^{\frac{4}{\alpha}}\lambda_{M_{\mathrm{s}}}^2}{16x}\right) \tag{21}$$

$$f_{I_4}(x) = \frac{\lambda_{I_4}}{4}\left(\frac{\pi}{x}\right)^{\frac{3}{2}}\exp\left(-\frac{\pi^4\lambda_{I_4}^2}{16x}\right) \tag{22}$$

with $\mu_{I_{\mathrm{m}},N}(t) = \log\mu_{I_{\mathrm{m}}}(t) - 0.5\log\left(1+\sigma_{I_{\mathrm{m}}}^2(t)/\mu_{I_{\mathrm{m}}}^2(t)\right)$ and $\sigma_{I_{\mathrm{m}},N}(t) = \log\left(1+\sigma_{I_{\mathrm{m}}}^2(t)/\mu_{I_{\mathrm{m}}}^2(t)\right)$, with $\mu_{I_{\mathrm{m}}}(t)$ and $\sigma_{I_{\mathrm{m}}}^2(t)$ given as $\mu_{I_{\mathrm{m}}}(t) = P_{\mathrm{mb}}\tau_{\mathrm{b}}\lambda_{\mathrm{m}}2\pi t^{-(\alpha-2)}/(\alpha-2)$ and

$$\sigma_{I_{\mathrm{m}}}^2(t) = \left(1+\frac{1}{M_{\mathrm{s}}K_{\mathrm{b}}}\right)\frac{\tau_{\mathrm{b}}\lambda_{\mathrm{m}}\pi P_{\mathrm{mb}}^2t^{-2(\alpha-1)}}{\alpha-2} \tag{23}$$

$\lambda_{M_{\mathrm{s}}} = (1-\tau_{\mathrm{b}})\lambda_{\mathrm{s}}\Gamma(1+2/\alpha)\prod_{i=1}^{M_{\mathrm{s}}-1}\left(i+\frac{2}{\alpha}\right)/\Gamma(M_{\mathrm{s}})$, and $\lambda_{I_4} = \lambda_{M_{\mathrm{s}}}\left(P_{\mathrm{sb}}/M_{\mathrm{s}}\right)^{\frac{2}{\alpha}} + \lambda_{M_{\mathrm{m}}}\left(P_{\mathrm{mb}}/M_{\mathrm{s}}K_{\mathrm{b}}\right)^{\frac{2}{\alpha}}$, and $\lambda_{M_{\mathrm{m}}} = \tau_{\mathrm{b}}\lambda_{\mathrm{m}}\Gamma\left(1+\frac{2}{\alpha}\right)\prod_{i=1}^{M_{\mathrm{s}}K_{\mathrm{b}}-1}\left(i+\frac{2}{\alpha}\right)/\Gamma(M_{\mathrm{s}}K_{\mathrm{b}})$.

Proof. See [17] for a detailed proof. □

By combining the previous results, we can now write the sum rate per area in a HetNet with wireless backhaul.

Theorem 1. *The sum rate per area in a heterogeneous network with wireless backhaul is given by*

$$\mathcal{R} = B\Big(K_{\rm m}\lambda_{\rm m} + K_{\rm s}\lambda_{\rm s}\Big)\Big\{A_{\rm m}\Big[\tau_{\rm m}R_{\rm m}^{\rm DL} + (1-\tau_{\rm m})R_{\rm m}^{\rm UL}\Big] + A_{\rm s}\Big[\tau_{\rm s}\min\Big\{R_{\rm s}^{\rm DL}, R_{\rm b}^{\rm DL}\Big\} + (1-\tau_{\rm s})\min\Big\{R_{\rm s}^{\rm UL}, R_{\rm b}^{\rm UL}\Big\}\Big]\Big\} \quad (24)$$

where B is the total available bandwidth, and $R_{\rm m}^{\rm DL}$, $R_{\rm m}^{\rm UL}$, $R_{\rm s}^{\rm DL}$, $R_{\rm s}^{\rm UL}$, $R_{\rm b}^{\rm DL}$, and $R_{\rm b}^{\rm UL}$ are given in (1), (2), (13), (14), (18), *and* (19), *respectively.*

Proof. See [17] for a detailed proof. □

4. NUMERICAL RESULTS

In this section, we provide numerical results to show the effect of several network parameters on the sum rate per area, and to give insights into the optimal design of a HetNet with wireless backhaul. Unless differently specified, the parameters are set as $P_{\rm mt} = P_{\rm mb} = 47.8$dBm, $P_{\rm sb} = P_{\rm st} = 23.7$dBm, $P_{\rm ut} = 17$dBm, $\sigma^2 = -96$dBm, $\tau_{\rm m} = \tau_{\rm s} = \tau_{\rm b} = 0.6$, $M_{\rm m} = 100$, $M_{\rm s} = 4$, $B = 20$MHz, $\lambda_{\rm m} = 10^{-6}{\rm m}^{-2}$, and $\alpha = 4$. We refer to *light load*, *medium load*, and *heavy load* conditions as the ones of a network with $\beta_{\rm m} = \beta_{\rm s} = \beta_{\rm b} = 0.25$, $\beta_{\rm m} = \beta_{\rm s} = \beta_{\rm b} = 0.5$, and $0.9 \le \beta_{\rm m}, \beta_{\rm s}, \beta_{\rm b} < 1$, respectively.

In Figure 2, we compare the sum rate per area of a HetNet under various load conditions and for different portions of the bandwidth allocated to the wireless backhaul. Figure 2 shows that the performance is highly sensitive to the bandwidth allocation, and that there is an optimal value of $\zeta_{\rm b}$ which maximizes the sum rate per area. The optimal value of $\zeta_{\rm b}$ increases as the load on the network increases, since SAPs need to forward more backhaul traffic to the MBSs to meet the rate demand. Figure 2 shows also shows that under spatial multiplexing, the network load has a significant impact on the sum rate per area. This indicates the importance of scheduling the right number of UEs per base station.

In Figure 3, we plot the sum rate per area of the network versus the number of SAPs per MBS. We consider three scenarios: (i) optimal bandwidth allocation, where the fraction of bandwidth $\zeta_{\rm b}$ for the backhaul is chosen as the one that maximizes the sum rate per area; (ii) fixed bandwidth allocation, where the bandwidth is equally divided as $\zeta_{\rm b} = 0.5$; and (iii) one-tier cellular network, where no SAPs or wireless backhaul are used at all, i.e., $\zeta_{\rm b} = 0$. Figure 3 shows that in a two-tier heterogeneous network there is an optimal number of SAPs associated to each MBS via the wireless backhaul that maximizes the sum rate per area. Such number is given by a tradeoff between the data rate that the SAPs can provide to the UEs, the interference generated, and the demand on the backhaul. This figure also indicates that a two-tier HetNet with wireless backhaul can achieve a significant rate gain over a one-tier deployment. However, this requires the backhaul bandwidth to be optimally allocated.

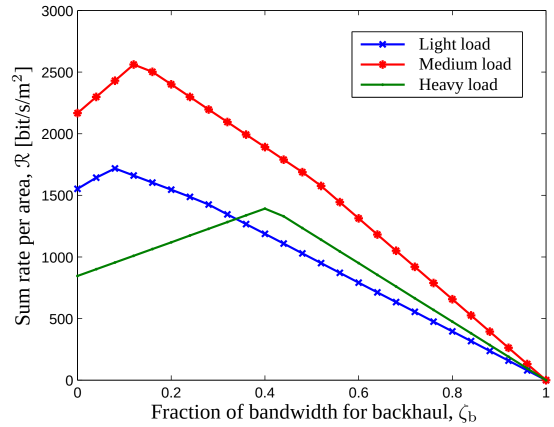

Fig. 2. Sum rate per area versus fraction of bandwidth $\zeta_{\rm b}$ allocated to the backhaul, under different load conditions.

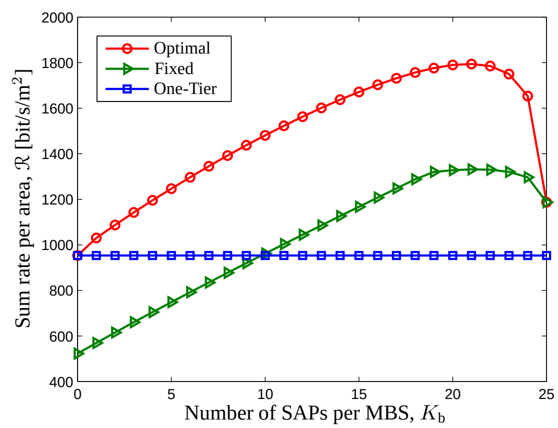

Fig. 3. Sum rate per area versus number of SAPs per MBS under various bandwidth allocation schemes.

5. CONCLUSION

In this work, we undertook an analytical study for the design of HetNets with wireless backhaul. We used a general model that accounts for uplink and downlink transmissions, spatial multiplexing, and resource allocation between radio access links and backhaul. Our results revealed that it is critical to control the network load to maintain a high sum rate per area. Moreover, a two-tier HetNet with wireless backhaul can achieve a significant performance gain over a one-tier deployment, as long as the bandwidth division between radio access links and wireless backhaul is optimally designed.

6. REFERENCES

[1] T. Q. S. Quek, G. de la Roche, I. Güvenç, and M. Kountouris, *Small cell networks: Deployment, PHY techniques, and resource management*, Cambridge University Press, 2013.

[2] J. G. Andrews, H. Claussen, M. Dohler, S. Rangan, and M. C. Reed, "Femtocells: Past, present, and future," *IEEE J. Sel. Areas Commun.*, vol. 30, no. 3, pp. 497–508, Apr. 2012.

[3] H. S. Jo, Y. J. Sang, P. Xia, and J. G. Andrews, "Heterogeneous cellular networks with flexible cell association: A comprehensive downlink SINR analysis," *IEEE Trans. Wireless Commun.*, vol. 11, no. 10, pp. 3484–3495, Oct. 2012.

[4] H. S. Dhillon, M. Kountouris, and J. G. Andrews, "Downlink MIMO HetNets: Modeling, ordering results and performance analysis," *IEEE Trans. Wireless Commun.*, vol. 12, no. 10, pp. 5208–5222, Oct. 2013.

[5] M. Wildemeersch, T. Q. S. Quek, C. H. Slump, and A. Rabbachin, "Cognitive small cell networks: Energy efficiency and trade-offs," *IEEE Trans. Commun.*, vol. 61, no. 9, pp. 4016–4029, Sep. 2013.

[6] H. S. Dhillon and G. Caire, "Wireless backhaul networks: Capacity bound, scalability analysis and design guidelines," *available as arXiv:1406.2738*, Jun. 2014.

[7] L. Sanguinetti, A. L. Moustakas, and M. Debbah, "Interference management in 5G reverse TDD HetNets: A large system analysis," *IEEE J. Sel. Areas Commun.*, vol. 33, no. 6, pp. 1–1, Mar. 2015.

[8] J.G. Andrews, "Seven ways that HetNets are a cellular paradigm shift," *IEEE Commun. Mag.*, vol. 51, no. 3, pp. 136–144, Mar. 2013.

[9] S. Singh, M. Kulkarni, A. Ghosh, and J. G. Andrews, "Tractable model for rate in self-backhauled millimeter wave cellular networks," *IEEE Trans. Wireless Commun.*, vol. 33, no. 10, pp. 2196–2211, Oct. 2015.

[10] D. C. Chen, T. Q. S. Quek, and M. Kountouris, "Backhauling in heterogeneous cellular networks: Modeling and tradeoffs," *IEEE Trans. Wireless Commun.*, vol. 14, no. 6, pp. 3194–3206, Jun. 2015.

[11] J. Zhao, T. Q. S. Quek, and Z. Lei, "Heterogeneous cellular networks using wireless backhaul: Fast admission control and large system analysis," *IEEE J. Sel. Areas Commun.*, vol. 33, no. 10, pp. 2128–2143, Oct. 2015.

[12] M. Sanchez-Fernandez, S. Zazo, and R. Valenzuela, "Performance comparison between beamforming and spatial multiplexing for the downlink in wireless cellular systems," *IEEE Trans. Wireless Commun.*, vol. 6, no. 7, pp. 2427–2431, Jul. 2007.

[13] H. Shirani-Mehr, G. Caire, and M. J. Neely, "MIMO downlink scheduling with non-perfect channel state knowledge," *IEEE Trans. Commun.*, vol. 58, no. 7, pp. 2055–2066, Jul. 2010.

[14] D. Lopez-Perez, M. Ding, H. Claussen, and A. H. Jafari, "Towards 1 Gbps/UE in cellular systems: understanding ultra-dense small cell deployments," *available as arXiv:1503.03912*, Mar. 2015.

[15] Q. H. Spencer, A. L. Swindlehurst, and M. Haardt, "Zero-forcing methods for downlink spatial multiplexing in multiuser MIMO channels," *IEEE Trans. Signal Process.*, vol. 52, no. 2, pp. 461–471, Feb. 2004.

[16] M. Joham, W. Utschick, and J.A. Nossek, "Linear transmit processing in MIMO communications systems," *IEEE Trans. Signal Process.*, vol. 53, no. 8, pp. 2700–2712, Aug. 2005.

[17] H. H. Yang, G. Geraci, and T. Q. S. Quek, "Energy-efficient design of MIMO heterogeneous networks with wireless backhaul," *available as arXiv:1509.05506*, Sep. 2015.

[18] S. Wagner, R. Couillet, M. Debbah, and D. T. M. Slock, "Large system analysis of linear precoding in correlated MISO broadcast channels under limited feedback," *IEEE Trans. Inf. Theory*, vol. 58, no. 7, pp. 4509–4537, Jul. 2012.

[19] G. Geraci, R. Couillet, J. Yuan, M. Debbah, and I. B. Collings, "Large system analysis of linear precoding in MISO broadcast channels with confidential messages," *IEEE J. Sel. Areas Commun.*, vol. 31, no. 9, pp. 1660–1671, Sep. 2013.

[20] G. Geraci, J. Yuan, and I. B. Collings, "Large system analysis of the secrecy sum-rates with regularized channel inversion precoding," in *Proc. IEEE Wireless Commun. Networking Conference*, Paris, France, Apr. 2012, pp. 533–537.

[21] R. Couillet and M. Debbah, *Random matrix methods for wireless communications*, Cambridge University Press, 2011.

[22] M. Haenggi, *Stochastic geometry for wireless networks*, Cambridge University Press, 2012.

[23] G. Geraci, H. S. Dhillon, J. G. Andrews, J. Yuan, and I. Collings, "Physical layer security in downlink multi-antenna cellular networks," *IEEE Trans. Commun.*, vol. 62, no. 6, pp. 2006–2021, Jun. 2014.